



ELSEVIER

Journal of Structural Geology 26 (2004) 625–636

**JOURNAL OF
STRUCTURAL
GEOLOGY**

www.elsevier.com/locate/jsg

Apparent boudinage in dykes

Paul D. Bons^{a,*}, Elena Druguet^b, Ilka Hamann^{c,d}, Jordi Carreras^b, Cees W. Passchier^c

^a*Institut für Geowissenschaften, Eberhard Karls Universität, Sigwartstraße 10, 72076 Tübingen, Germany*

^b*Departament de Geologia, Universitat Autònoma de Barcelona, 08193 Bellaterra (Barcelona), Spain*

^c*Tektonophysik, Institut für Geowissenschaften, Johannes Gutenberg-Universität, 55099 Mainz, Germany*

^d*Now at: Alfred-Wegener-Institut, Columbusstrasse, 27568 Bremerhaven, Germany*

Received 3 February 2003; received in revised form 1 September 2003; accepted 3 November 2003

Abstract

Intrusive rocks may be arranged in the form of strings of lenses or beads, as found on the Cap de Creus Peninsula, NE Spain, and in the South Finland Migmatite–Granite Belt. These structures first appear to be the result of stretching and boudinage of intrusive sheets or dykes. However, closer examination reveals that they are not boudins, but are instead primary intrusive structures. A detailed study was performed on a swarm of pegmatite intrusions at Cap de Creus. Layering is often continuous between beads, and, in some cases, individual beads exhibit a very irregular shape. These observations are shown to be incompatible with an origin by boudinage. Analogue experiments were used to test the effect of the two models (boudinage and emplacement) on the structures around beads, and show that an emplacement model of local expansion and collapse of magmatic sheets is the most compatible with field observations. Such structures can only form when dykes intrude hot rocks, when magma solidifies slowly enough to allow enough ductile flow of the wall rock to accommodate the formation of the beads. The fact that the pegmatite bead strings are not boudins has repercussions for the interpretation of the deformation at Cap de Creus and necessitates caution in the interpretation of deformation based on apparent boudins in intrusive rocks in other areas.

© 2004 Elsevier Ltd. All rights reserved.

Keywords: Pegmatite; Dykes; Boudinage; Emplacement; Analogue experiments

1. Introduction

Magmatic dykes form by the intrusion of magma into a planar fracture and subsequent freezing of the magma inside the open fracture (Spence and Turcotte, 1985; Rubin, 1993; Petford et al., 2000; Bons et al., 2001). After solidification, the dykes normally have a different rheology from their host rocks. Tectonic extension of dykes that are more competent than their host rocks can lead to boudinage (Cloos, 1947; Ramberg, 1955; Ramsay, 1967; Hanmer, 1986; Price and Cosgrove, 1990; Goscombe and Passchier, 2003). Here the competent dyke is segmented into a series of blocks or lenses. The surrounding foliation may fold inwards into the boudin necks. These boudins form a valuable source of information on strain and other aspects of finite deformation and flow (Mawer, 1987; Goldstein, 1988; Swanson, 1992; Lacassin et al., 1993; Goscombe and Passchier, 2003). In Northeast Spain and South Finland, pegmatitic and mafic

intrusions in the form of strings of blocks and lenses closely resemble stretched and boudinaged dykes (Carreras and Druguet, 1994). However, this paper describes and explains these structures as primary emplacement structures that are not the result of stretching. Description of their shape and comparison with analogue models sheds some light on ascent and emplacement of magma. We show that erroneous attribution of such dykes as boudinaged structures can lead to errors in regional tectonic interpretations.

2. Boudin-like intrusions from the Cap de Creus Peninsula

2.1. Geological setting of Cap de Creus

The Cap de Creus Peninsula (Fig. 1) forms the eastern-most outcrop of the Variscan Axial Zone of the Pyrenees (Fig. 1a; Barnolas and Chiron, 1996; Ábalos et al., 2002). Only the most relevant points of the local geology are described here, and the readers are referred to Carreras and

* Corresponding author. Tel: +49-7071-2976469; fax: +49-7071-5059.
E-mail address: paul.bons@uni-tuebingen.de (P.D. Bons).

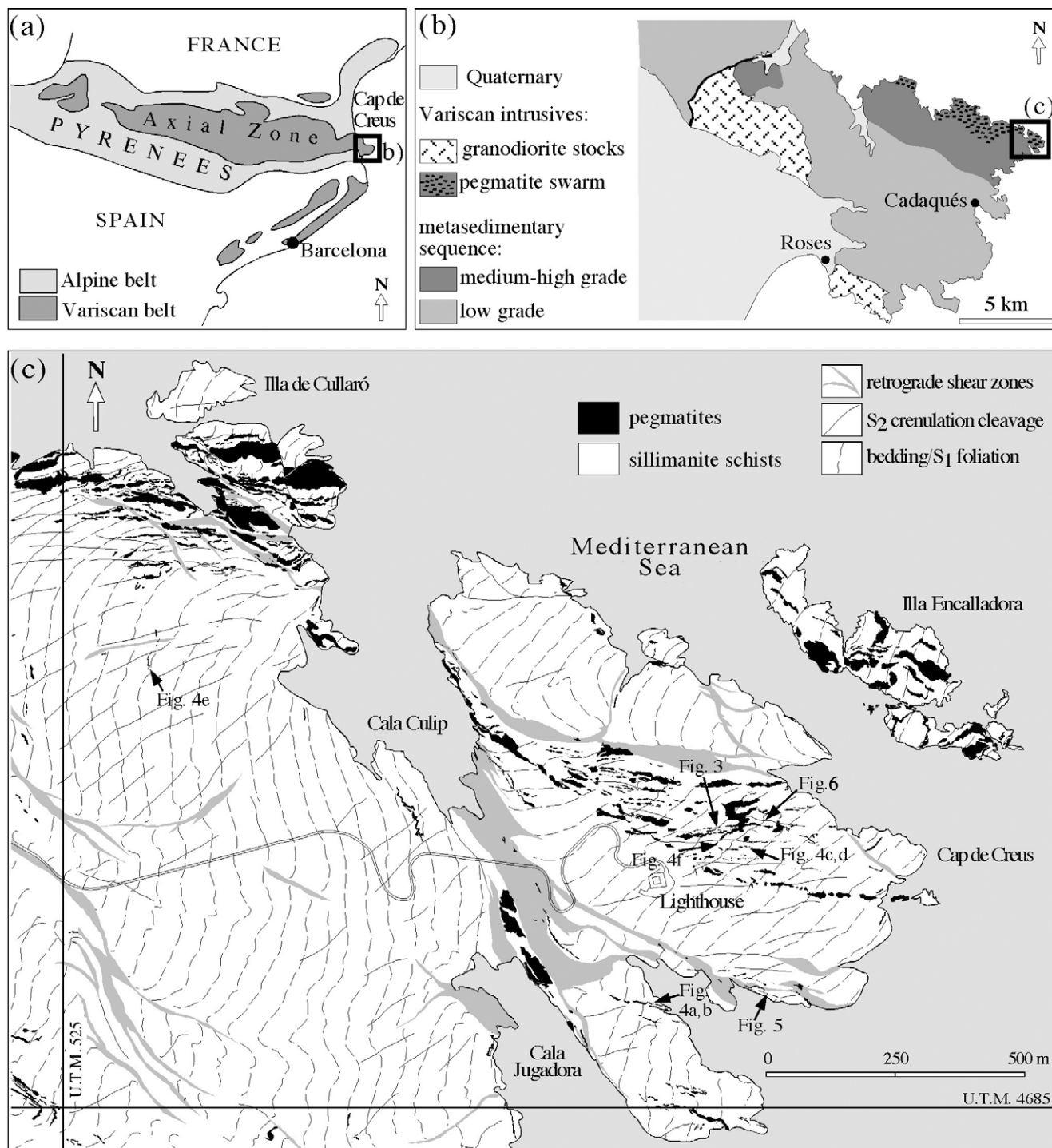


Fig. 1. Geological setting of pegmatite intrusions in Cap de Creus. (a) Location of the Cap de Creus peninsula in the eastern Variscan Axial Zone of the Pyrenees. (b) Geological sketch of the Cap de Creus peninsula with location of the study area. (c) Structural map of the study area, after Druguet (1997). Dashed lines represent traces of the steeply dipping, composite bedding/ S_1 , which strikes N–S in the south-west corner of the area and is rotated clockwise 45–70° around the lighthouse and up to 90° south of Illa de Cullaró.

Druguet (1994), Druguet et al. (1997), Druguet and Hutton (1998), Druguet (2001) and Carreras (2001) for more extensive descriptions. Alternating layers of Neoproterozoic or Cambro-Ordovician metapelites and metapsammites form the dominant lithology, which was metamorphosed up to upper-amphibolite facies with local onset of partial

melting during the Variscan Orogeny. Metamorphic grade decreases from north to south (Fig. 1b).

Our interpretation of the tectonic history as given here has been modified from previous reconstructions after recognition that segmented pegmatite veins represent intrusive features, and not boudins. A layer-parallel

foliation (S_1) developed during the first stage of prograde metamorphism. Bedding and S_1 form a composite foliation, henceforth termed $S_{0/1}$. The second deformation phase commenced before peak metamorphism, produced asymmetric steeply-inclined S-shaped folds in bedding and early quartz veins, and a steeply-dipping crenulation cleavage (S_2) (Fig. 2a). The N-striking S_1 and a NE-striking S_2 in the south were subsequently rotated clockwise by up to $\sim 90^\circ$ in the northern part of the area (Figs. 1c and 2b). The latter rotation indicates an ESE–WNW oriented dextral shear component of deformation. Pegmatites intruded syn- to post-peak metamorphism before, or during this dextral rotation, and are most abundant in the north of the area, where rotation of existing foliations is most pronounced. Geochemical analyses point towards an anatectic origin for the pegmatites, which would be derived from the metasedimentary country rocks (Damm et al., 1992). This is a common situation in the Variscan rocks of the Pyrenees, where anatectic cores of metamorphic domes are surrounded by ‘perianatectic’ domains with abundant pegmatites (Autran et al., 1970). However, Alfonso et al. (2003) argue that the pegmatites are derived from fractionation of common parental granitoid magma. Late anastomosing shear zones cross-cut the area (Figs. 1c and 2c) and can be recognized by intense mylonitisation and retrogression to greenschist facies mineral assemblages (Carreras, 2001).

2.2. Morphology of pegmatite intrusions at Cap de Creus

Most pegmatite intrusions currently lie in a steep E–W to NW–SE orientation, where the dominant $S_{0/1}$ foliation is oriented approximately NE–SW (Fig. 1c). The characteristic shape of pegmatite intrusions in horizontal exposures is a series of elongate blocks, pods, or lenses that vary in size from less than a metre to tens of metres in length (Figs. 3, 4a–c and 5). Individual pegmatite bodies are connected by thin, pegmatite-filled seams with occasional lenses and flame-shaped apophyses of pegmatite (Fig. 4b–d). Some seams are completely closed. In outcrop, the pegmatites thus look like beads that are connected by a string (the seam), which is why we henceforth use the term ‘bead string’ to describe them. Bead strings can be hundreds of metres long. In some cases, the structure changes along its length to a more regular sheet-like geometry that gradually tapers to a <millimetre-wide tip over tens of metres (Fig. 6). This sheet always lies at the eastern end of a string and the transition from beaded habit to the sheet occurs when the average width of beads and sheet are about 10 cm. The sheets are occasionally slightly folded (Fig. 6b) or boudinaged, but in general appear little stretched, nor shortened. Some minor stretching and shortening along pegmatite bead strings are indicated, respectively, by occasional quartz precipitate in pressure-shadow locations and minor folding of connecting seams.

The three-dimensional shape of the pegmatite bead strings is visible only in a few steep exposures (Fig. 7).

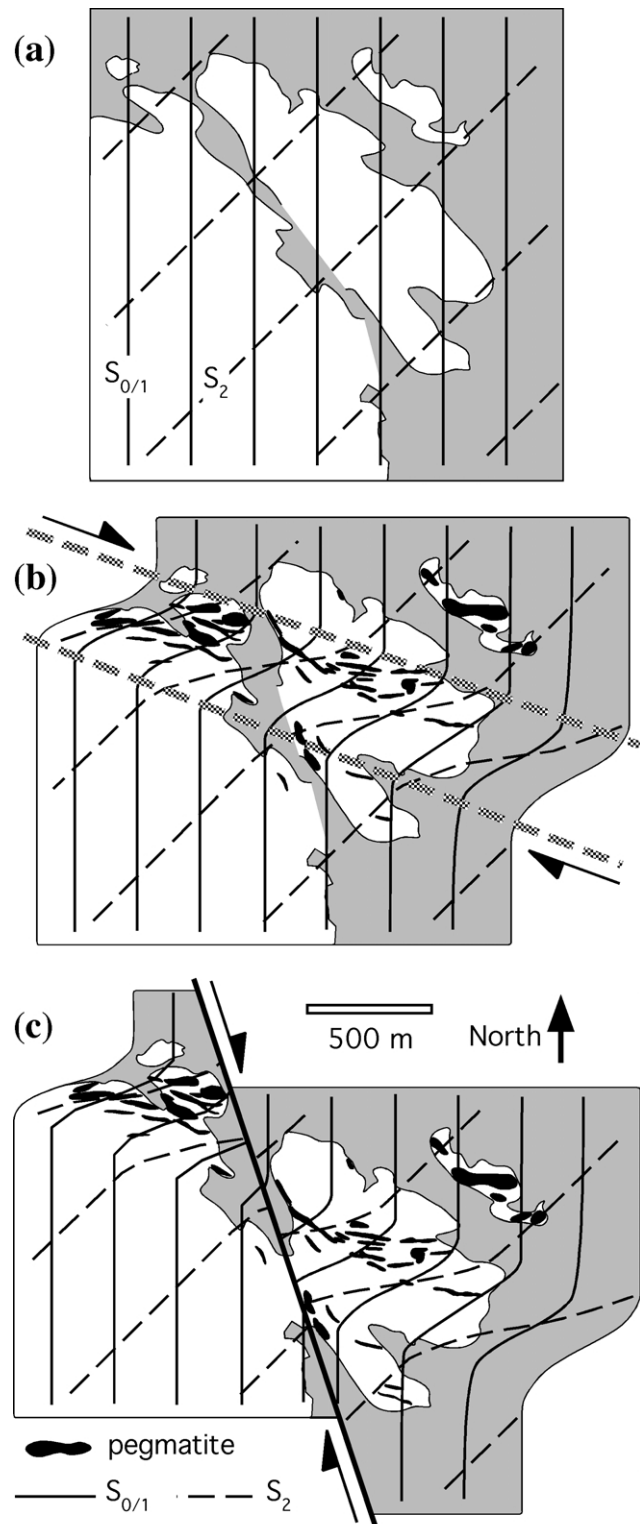


Fig. 2. Simplified tectonic history and reconstruction of the area shown in Fig. 1c. (a) Situation before pegmatite intrusion. The steep composite $S_{0/1}$ trends N–S, while S_2 is striking NE–SW. (b) Situation after pegmatite intrusion and dextral shear along a WNW–ESE-trending zone, which sheared and rotated $S_{0/1}$ and S_2 . (c) Current situation after dextral shearing along a major retrograde shear zone complex that runs through Cala Culip and Cala Jugadora. Only the main retrograde shear zone is shown, but many more dissect the area.

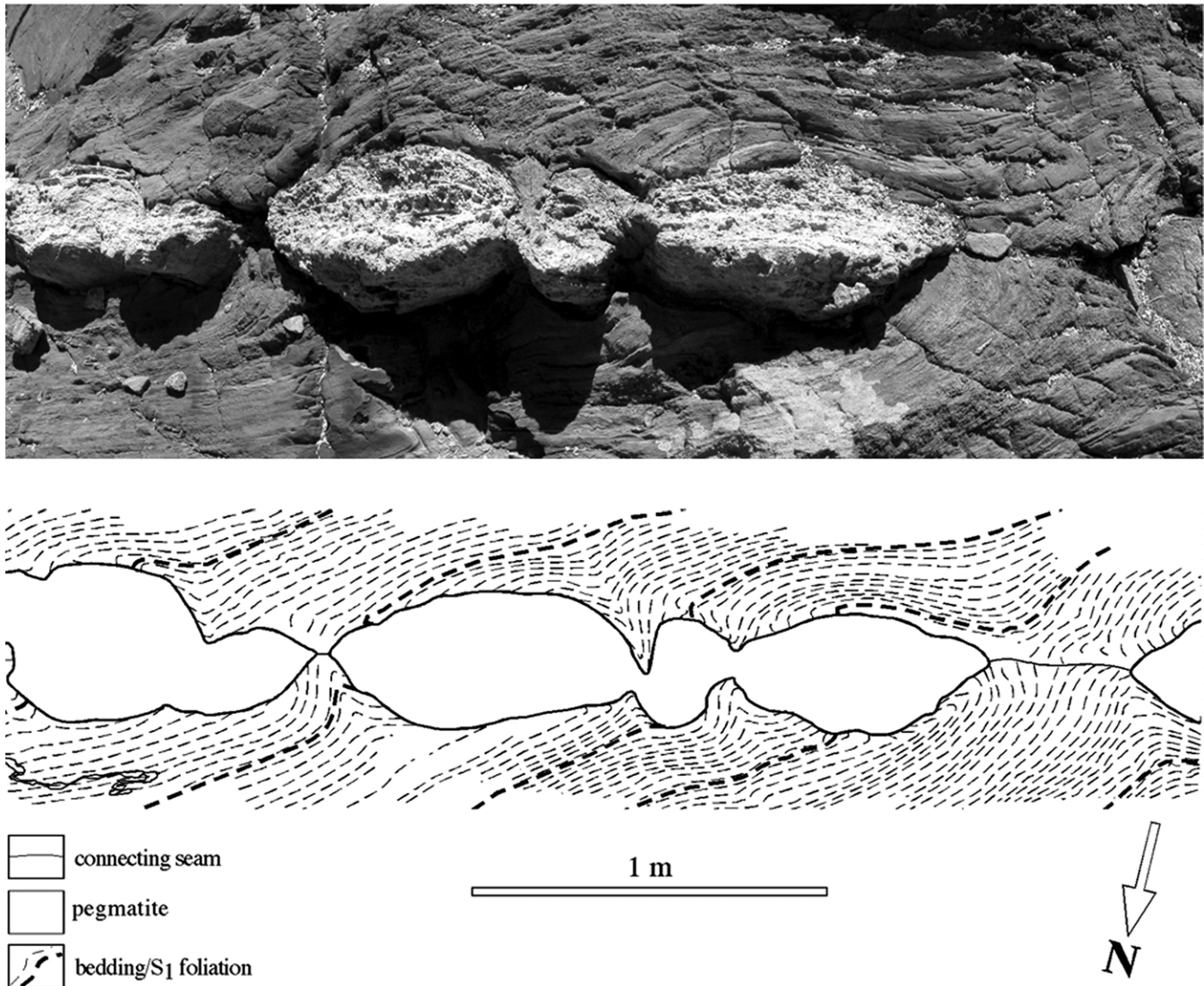


Fig. 3. Pegmatite bead string from Cap de Creus (plane view photograph and line drawing). S_{01} is deflected around the beads and cuts across the space between the right-most two beads. Deflection folds show an 'S'-shaped asymmetry. Location shown in Fig. 1.

Where visible, beads tend to be longer in the vertical than in the horizontal direction. Their average shape is thus that of a short and flattened rod. The direction of maximum elongation can vary from vertical to about 45° east-plunging. Sometimes, beads are not fully separated, but show pinch-and-swell like geometries.

Pegmatite bead strings and small veins commonly have a millimetre–10 cm wide alteration rim that is strongly enriched in tourmaline, and in which the main foliation is usually close to perpendicular to the vein/string orientation (Fig. 4f). Further away from the rim, the foliation tends to have $<45^\circ$ angles with the pegmatite. These tourmaline-rich rims appear to have been relatively rigid and have preserved the original pre-deformation relationship between vein/string and foliation orientations (Druguet et al., 1997; Passchier, 2001).

Sedimentary layering and crenulation cleavage (S_2) are

folded and deflected around beads in a characteristic way (Figs. 3, 4c and 5c), which resembles folding around real boudins (Ghosh and Sengupta, 1999; Goscombe and Passchier, 2003). However, between beads, layering is continuous across the connecting seams and is little deflected (Figs. 4c and 5b). Deflection of the main foliation always has a monoclinic symmetry, especially where main foliation and bead strings make a small angle (Figs. 3 and 5c).

Two other, but minor, populations of pegmatite intrusions are found: one is approximately horizontal, and the other steeply N–S-striking. They are generally a few decimetres to more than a metre wide and both populations occur as non-beaded dykes and are folded (Fig. 4e). When differently oriented pegmatites intersect, one clearly cuts through the other. The pegmatites do therefore not branch out into different orientations. We did not, however, find any

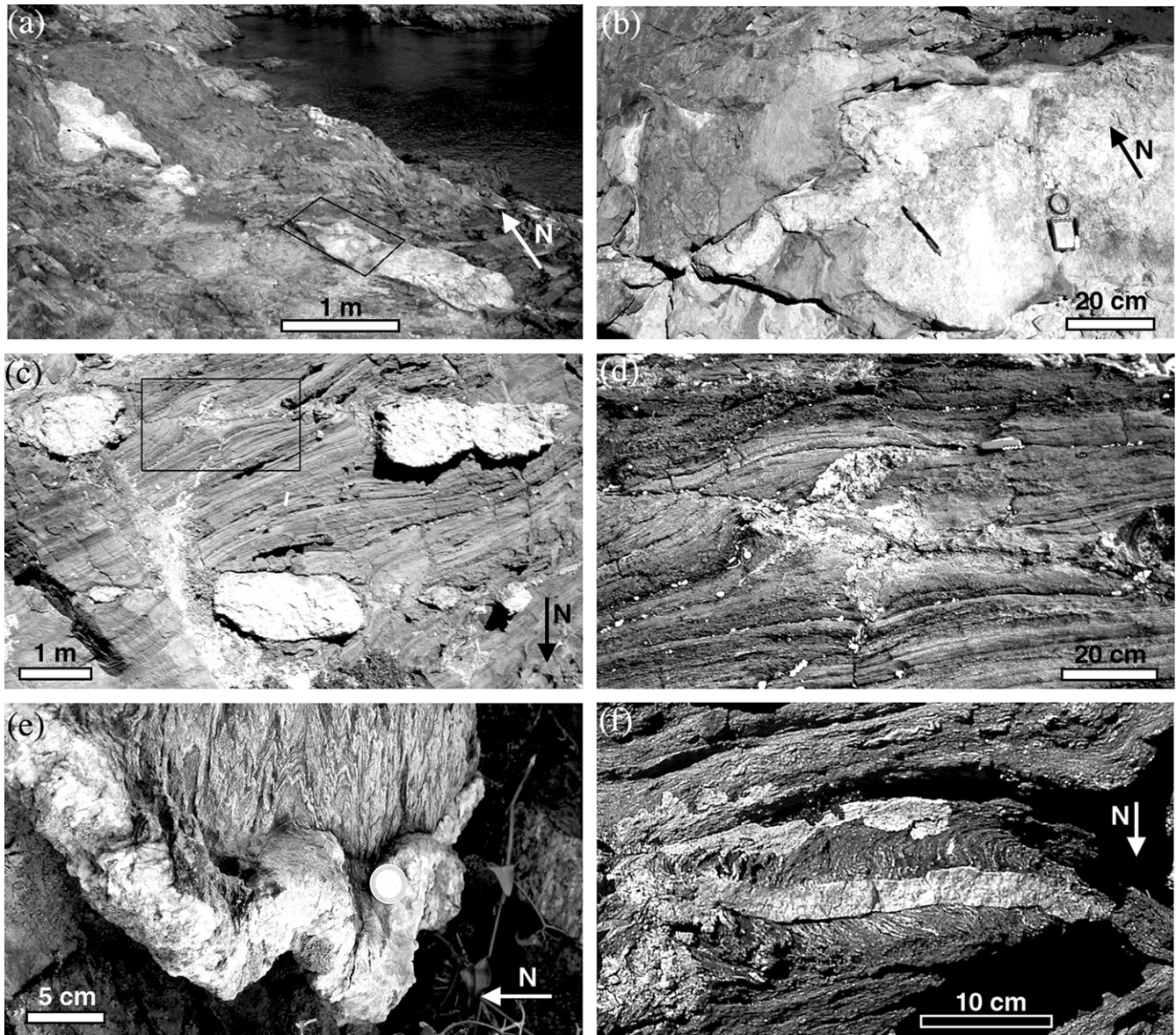


Fig. 4. Field photographs of pegmatite intrusions at Cap de Creus. (a) Two beads from a bead string. Rectangle shows outline of (b). (b) Individual box-shaped pegmatite bead, connected to decimetre-wide seam at the left. (c) Two parallel bead strings viewed from above. The $S_{0/1}$ foliation clearly cuts across the wide spacing between the beads. Rectangle shows outline of figure (d). (d) Flame-like apophyses emanating from thin seam between beads. (e) Folded NE-trending pegmatite sheet. The sheet cuts earlier D_2 folds in laminated $S_{0/1}$. (f) Tourmaline rich rim developed around a pegmatite vein. $S_{0/1}$ is preserved in the rim at a high angle to the pegmatite walls. All locations shown in Fig. 1.

systematic age relationships between the different populations, suggesting that all pegmatites intruded during the same event.

3. Bead strings in the South Finland Migmatite–Granite Belt

To show that the bead strings are not a unique feature of Cap de Creus, nor of pegmatites, we briefly describe two examples from the South Finland Migmatite–Granite Belt, which forms a roughly E–W striking, 50–100-km-wide belt of amphibolite to granulite-facies metasedimentary rocks

and mostly granitoid intrusions (Ehlers et al., 1993). Polyphase deformation, metamorphism, migmatitisation and magmatic activity ranges in age from about 1890 to 1800 Ma (Ehlers et al., 1993; Lindroos et al., 1996). Magmatic activity included dyke-like intrusion of minor mafic magmas and abundant pegmatites into high metamorphic grade (up to anatexis) metasediments and granitoid complexes. Pegmatite intrusions into migmatites often show bead-geometries, similar to those found at Cap de Creus (Fig. 8a). Mafic intrusions into (probably) partially molten granitoids also show the same geometries with irregular lenses that are connected by thin seams (Fig. 8b).

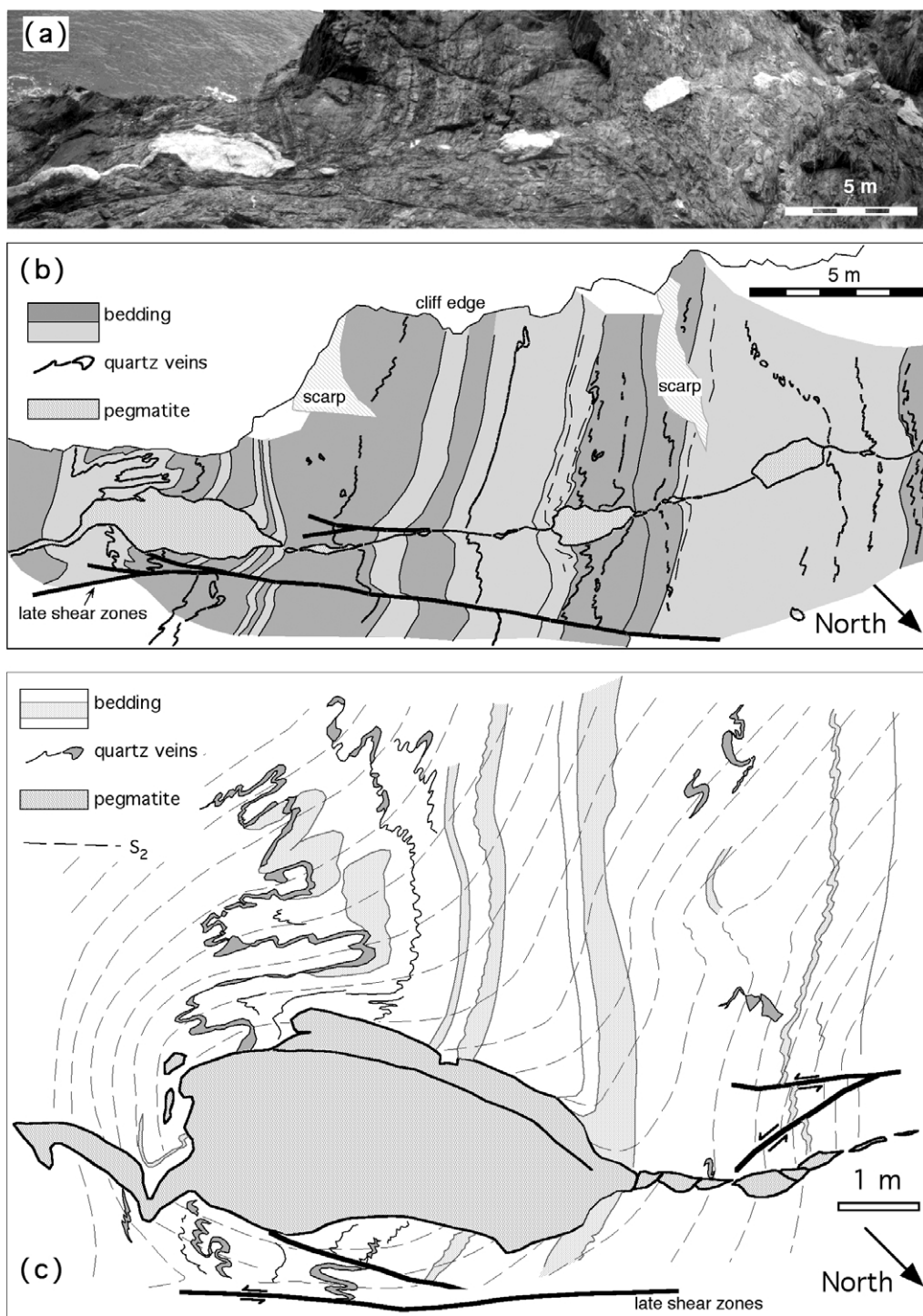


Fig. 5. (a) Pegmatite bead string exposed on NE-sloping coastal outcrop. (b) Drawing of the pegmatite bead string, shown in (a), highlighting the continuity of sedimentary layering between beads, which is incompatible with boudinage. If the beads were formed by boudinage, the spacing would indicate a stretching factor of more than two. (c) Detail of left-most bead in (b), showing the deflection of S_2 - and D_2 -folded sedimentary layering and quartz veins around the bead. Location shown in Fig. 1.

4. Interpretation of pegmatite structures

4.1. Boudinage versus emplacement structures

The pegmatite bead strings have earlier been interpreted as boudins resulting from stretching after emplacement

(Carreras and Druguet, 1994). From the ratio of the total length of a bead string and the total length of individual pegmatite beads, one obtains stretch values between 1.2 (for thin) and >2 (for thick) pegmatite bead strings (Fig. 5). However, bead strings have a number of characteristics that are difficult to explain by boudinage (see below), and we

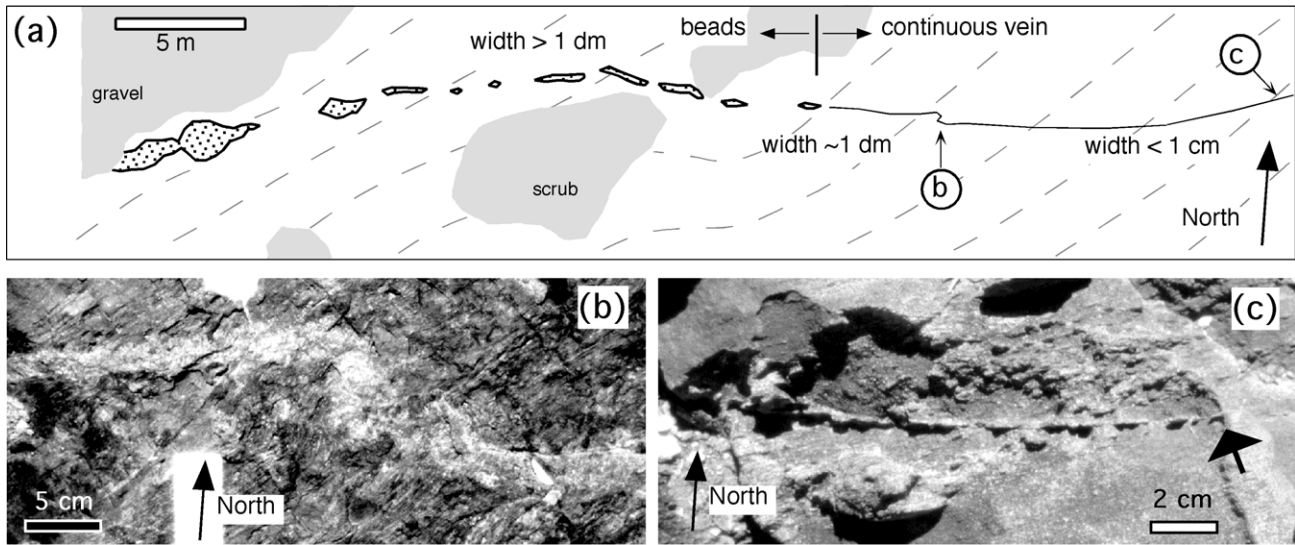


Fig. 6. (a) Drawing of the transition of a bead string (width > 10 cm) to a thin continuous seam (width < 10 cm down to 1 mm). Location shown in Fig. 1. (b) Detail of minor folding of the seam. (c) Detail of the narrow tip of the seam; broad arrow points at tip.

now propose that the bead strings are primary emplacement structures. In this model, the beads form from an intruding pegmatite dyke, which then falls apart into beads by local collapse and inflation of the dyke (Fig. 9). In this case no bead string-parallel stretching is necessary.

We used analogue experiments with a shear box described by Piazzolo et al. (2001) to test the effect of the two models on the structures around and between individual beads. The transparent linear viscous polymer polydimethylsiloxane (PDMS; Weijermars, 1986; ten Grotenhuis et al., 2002) was used as an analogue of the host rock of the pegmatites. To simulate boudinage, we deformed a 215×175 mm sample of PDMS with three aligned rectangular neutrally buoyant rigid boxes (4.7×1.4 cm) in pure shear parallel to the row of boxes, at a stretching rate of $6.0 \times 10^{-6} \text{ s}^{-1}$ (Fig. 10a). To simulate local dyke inflation, we inserted 35 playing cards (44×65 mm) one by one vertically into the PDMS with intervals of 2 min (Fig. 10c). We only modelled the formation of one isolated bead by inflation, effectively assuming that beads are separated far enough to avoid mutual interaction, as would be applicable to the bead string shown in Fig. 5. It should be noted here that local expansion of a dyke imposes the same effective finite strain field on the adjacent host rock as local collapse (Fig. 10e). After the experimental bead or boudins were

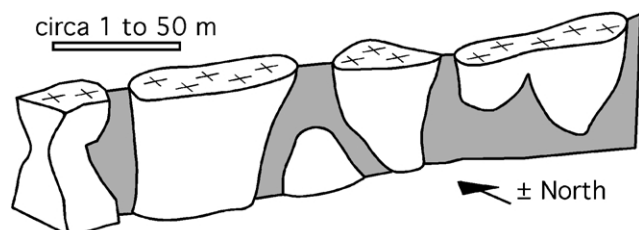


Fig. 7. Schematic drawing of the three-dimensional geometry of a bead string. Individual beads are generally elongated in the vertical direction.

made, we applied a dextral simple shear of $\gamma \approx 1$ at a shear strain rate of $2.1 \times 10^{-4} \text{ s}^{-1}$ (Fig. 10b and d). The flow field and finite strain around the experimental beads could then be determined from a grid that was drawn on the PDMS. This grid can be used to determine the deflection pattern of any passive marker, such as a foliation. Fig. 11 shows the resulting structures for three initial orientations of a passively deforming foliation: 0° , 45° and 90° to the initial bead string.

In the case of boudinage (Fig. 11a), one can see that a high strain zone spans the entire area between boudins. This is the most crucial difference with the inflation model, where the highest strain occurs at the corners of an expanding bead and decreases away from the corners (Fig. 11b). If beads are far apart, little strain is induced halfway between the beads. The latter model is therefore most compatible with the field observations where sedimentary layers and crenulation cleavage continue between beads, with only minor deformation where these are cut by the seam (Figs. 3, 4c and 5). In the case of boudinage, layers do not run up to the seam in boudin necks. Furthermore, the flame-like apophyses between the beads (Fig. 4d) argue against an origin by boudinage. These apophyses do not have the shape of torn-off pieces of boudins and often appear compositionally slightly different from the main beads. This would suggest that these apophyses are original magma intrusions emanating from the seams between the beads.

A further argument against boudinage is the fact that some thin (< 10 cm) continuous pegmatite veins or thin parts of bead-string veins are not boudinaged, and may even be slightly shortened (by folding; Fig. 6b). In a stretching field, these veins should have boudinaged too, if parallel and thicker pegmatites were boudinaged. Finally, there is no sub-horizontal stretching lineation parallel to pegmatite

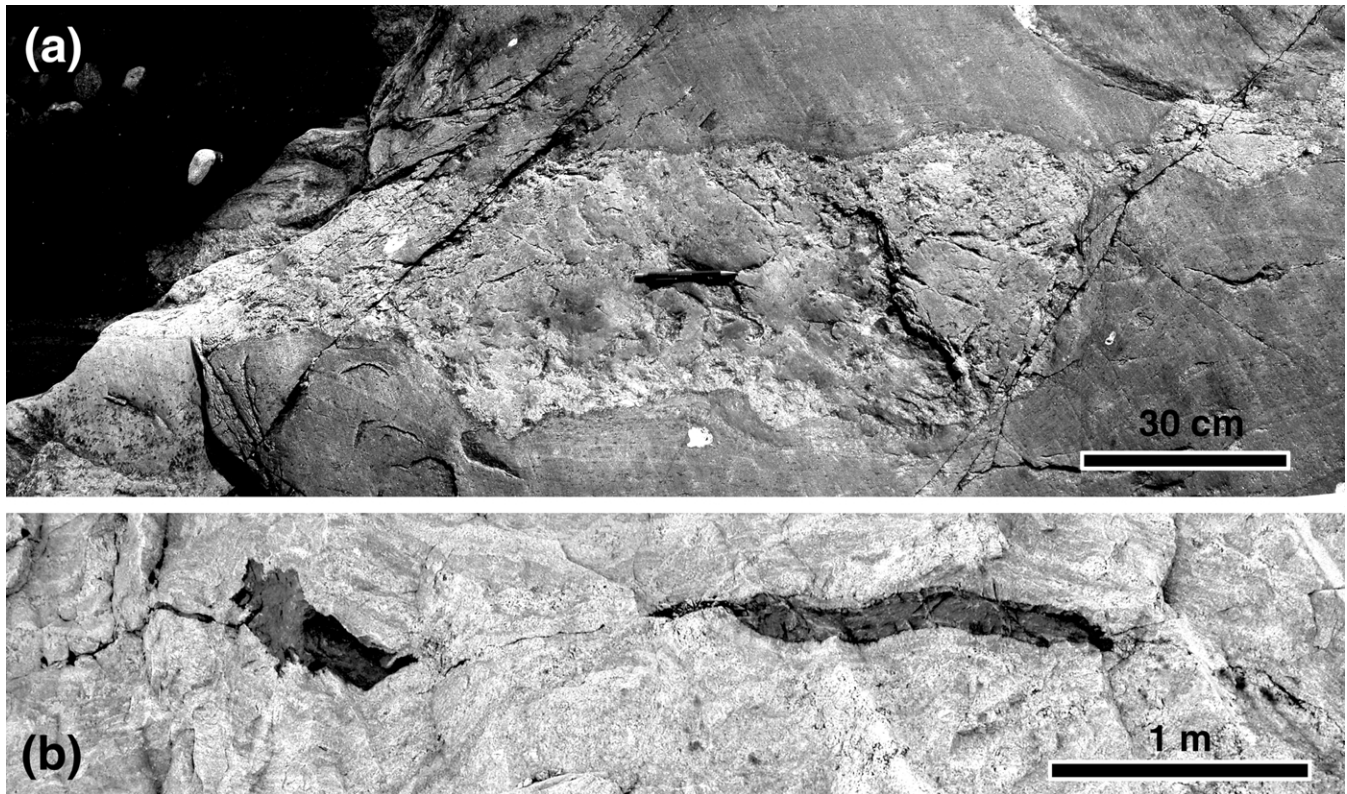


Fig. 8. (a) Pegmatite bead intruded into migmatite at the classical Kopparnäs outcrops, described by Sederholm (1926). Oblique stripes are glacial striae. Coordinates: E 24°15.20', N 60°2.59'. (b) Mafic bead string intruded into a partially molten migmatite and granite complex. Two irregularly shaped metre-sized beads are connected by a thin seam. Road cut at the intersection of road number 2200 and the Turku–Helsinki freeway, near Vättilä. Coordinates: E 22°22.83', N 60°25.49'.

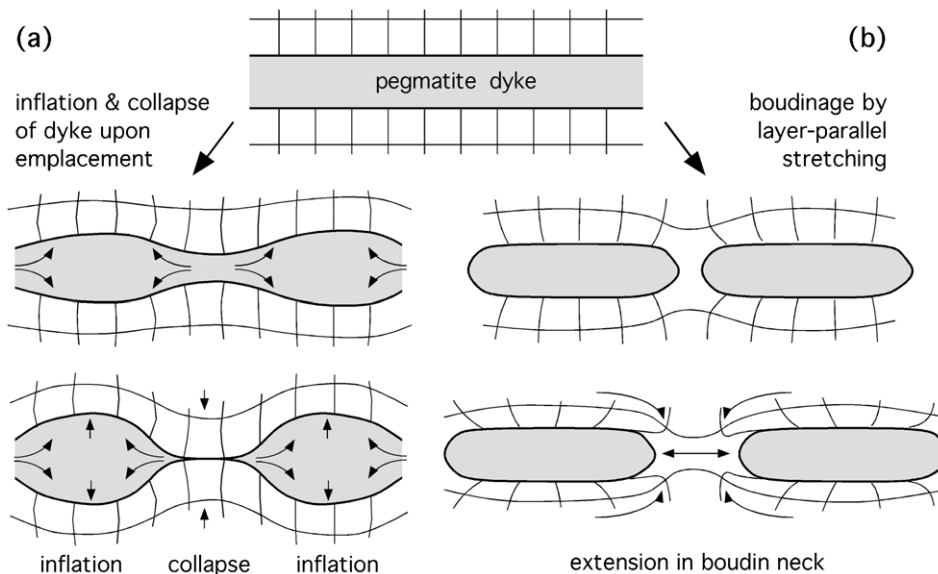


Fig. 9. Schematic illustration of the two models that may lead to boudin/bead string geometries. (a) Collapse and inflation of a pegmatite dyke upon emplacement, without any dyke-parallel stretching. (b) Boudinage of a solidified pegmatite dyke, due to dyke-parallel stretching.

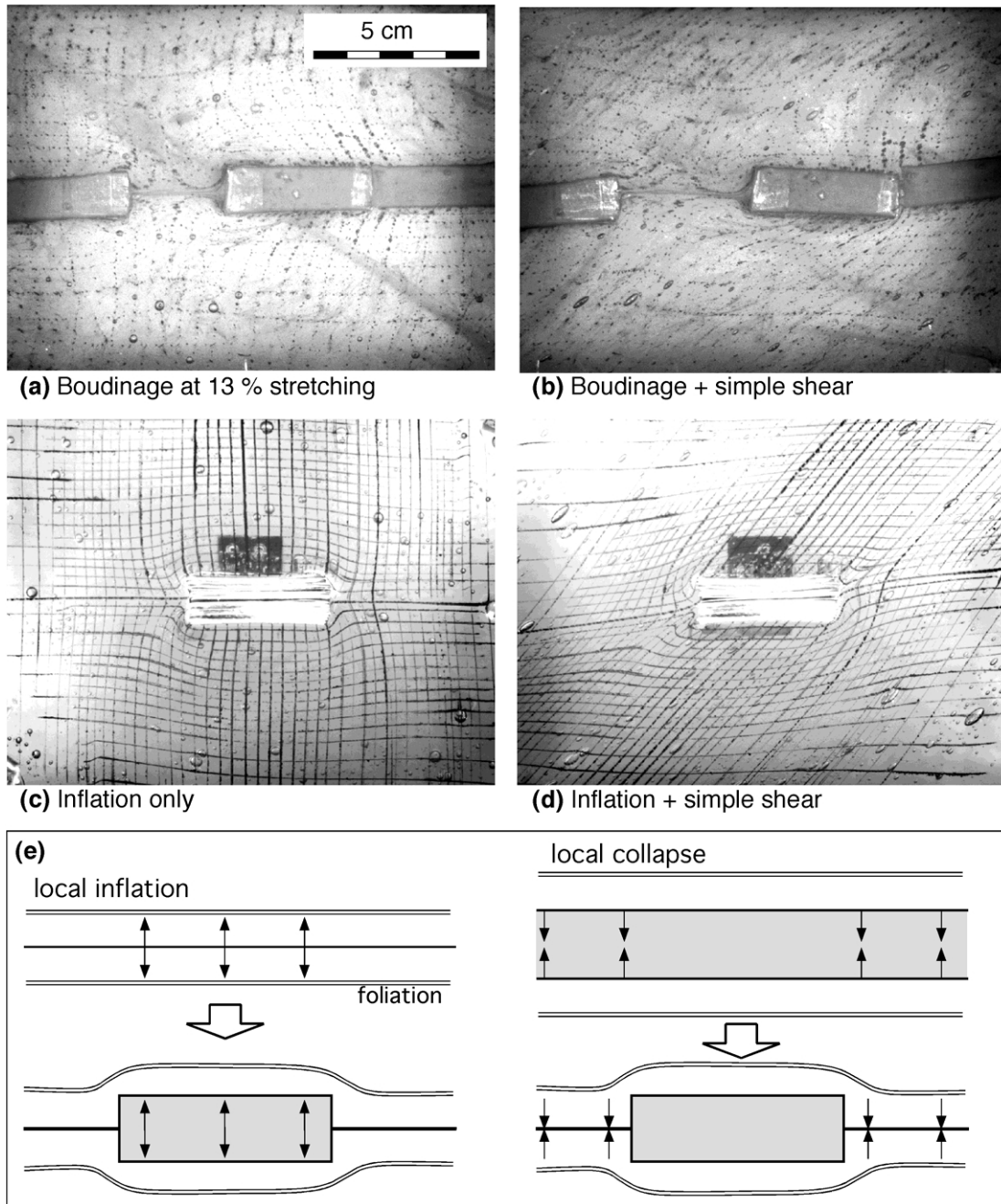


Fig. 10. (a) Photographs of shear box experiments. All photographs are focussed on the free surface of the PDMS sample, on which a passive grid was drawn to determine the strain field. (a) Boudinage induced in a layer composed of three rigid boxes, embedded in ductile PDMS. (b) The same as (a), but after application of a dextral shear strain of $\gamma \approx 1$. (c) Local inflation of a thin sheet, simulated by sequential insertion of 35 playing cards into PDMS. (d) The same as (c), but after application of a dextral shear strain of $\gamma \approx 1$. The dark rectangle in the background is a support to avoid sinking of the cards. (e) Local inflation and local collapse both give identical deflection patterns in the matrix, because boundary conditions for the matrix are effectively identical. The deflection pattern is purely derived from the relative movements of the inflating/non-inflating or collapsing/non-collapsing boundary between dyke and matrix.

dykes and bead strings, not even in the seams between beads.

4.2. Monoclinic symmetry

Without shearing, a monoclinic symmetry of deflection of the foliation around pegmatites only develops if the foliation was originally oblique to the boudinaging layer or

bead string (Fig. 11). However, the tourmaline-rich rims indicate that foliation was originally at a large angle to the pegmatite bead-strings and veins (Druguet et al., 1997; Passchier, 2001; Fig. 4f). The fact that thin tips of bead strings show, at the most, only minor stretching or shortening but no dominant extension suggests that regional horizontal stretch parallel to the bead strings was approximately zero. The foliations (bedding and cleavage) must

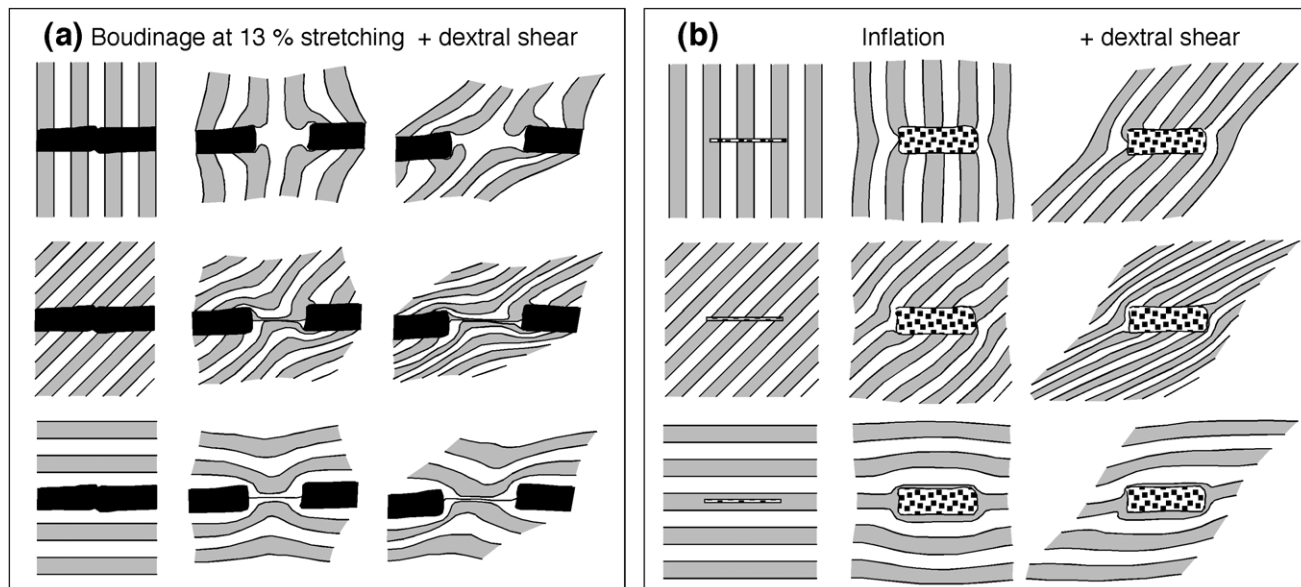


Fig. 11. Drawings of geometries of hypothetical layering around boudins and beads, derived from the strain fields (deformed grids) that were recorded in the experiments (Fig. 10). The effect of boudinage (a), and inflation (b) are shown for layering initially perpendicular, oblique (45°) and parallel to the boudin or bead string. Left column: starting position. Middle column: deflections after boudinage or inflation. Right column: deflections after application of a dextral shear strain of $\gamma \approx 1$.

therefore have rotated several tens of degrees relative to each other, without significant stretching or shortening parallel to the pegmatite veins or strings. Vein- or string-parallel dextral simple shearing, or transpression with minor vertical extension, are flow fields compatible with these observations. In such deformation fields, the vein or string would neither stretch nor shorten, but foliations in other orientations would rotate synthetically with the shearing. This indicates that the rocks experienced a dextral shear strain component in the order of $\gamma \approx 1-2$, with a roughly WNW-trending shear plane (Fig. 2b). This produces a monoclinic symmetry, with S-shaped deflections, even in cases where the original emplacement structure had a higher symmetry, with the foliation at $\sim 90^\circ$ to the bead strings (Fig. 11).

4.3. Emplacement mechanism

Assuming that the bead strings formed by local inflation and/or collapse of a dyke, we first summarise relevant observations before discussing possible mechanisms by which this process may have occurred:

1. Bead strings end in a narrow crack-like tip.
2. Pegmatite intrusion occurred at peak-metamorphic conditions, where the host rock was close to anatexis (Druguet and Hutton, 1998; Druguet, 2001) and able to flow ductily around the beads.
3. Different pegmatite orientations show cross-cutting relationships, but no branching.

4. The dominant roughly E-trending pegmatite population is beaded, whereas other populations are not.

The two currently popular and relevant models for transport of small volumes of magma are (1) propagation of individual hydrofractures or dyking, and (2) pervasive flow through connected fractures (Spence and Turcotte, 1985; Emerman and Marrett, 1990; Rubin, 1993; Weinberg, 1999; Petford et al., 2000; Bons et al., 2001; Bons and van Milligen, 2001). Pervasive flow can be discounted for the emplacement stage of dyke formation at Cap de Creus, as most bead strings are parallel and do not connect, and relative differences in age are found where different orientations do intersect. The different dykes were therefore not all actively transporting magma at the same time. Transport in propagating hydrofractures appears the most suitable transport model here, although the current morphology must have been modified by ductile emplacement processes. At low levels in the crust, ductile conditions promote the intrusion of pegmatites with lenticular to bulbous shapes, compared with tabular pegmatite dykes emplaced in the upper crust where brittle conditions prevail (Brisbin, 1986). Hydrofracture propagation is a brittle-elastic process, which is envisaged to occur in thin narrow fractures (Lister and Kerr, 1991; Petford et al., 1993). To our knowledge, no dyking model exists that predicts bead-like structures to form during fracture propagation and magma transport. We therefore propose that the pegmatitic magma ascended in thin cracks, of which the narrow tapered tails that were observed may be representative (Fig. 6a). The formation of the bead structures must then have occurred after magma had intruded. The dominance of narrow

Table 1

Main characteristics to distinguish bead strings from boudins that formed due to stretching of a layer or dyke

	Bead strings	Boudin trains
Strain distribution	Most intense strain and deflection of foliation is around the beads, especially at corners. Strain decreases away from beads (Fig. 11)	Most intense strain and deflection of foliation is between boudins. Between boudins, strain intensity does not decrease away from boudins
Oblique bedding and foliations	Bedding or foliations at an angle to bead strings are continuous across space between beads (Fig. 5)	Bedding or foliations at an angle to boudin trains cannot cross boudin necks
Connecting seams	Beads are connected by a thin connecting seam, showing little or no internal deformation (Figs. 4 and 8)	Any connecting seam would consist of strongly deformed material that was sheared away from the boudins
Apophyses	Flame-like igneous apophyses may emanate from connecting seam (Fig. 4d)	No igneous apophyses

crack-like tips of bead strings at one end (east), suggests that magma accumulated towards the other end (west), probably the top of the fracture, once magma transport came to a halt due to freezing or insufficient magma supply. Beads would then develop as the result of mechanical instabilities, the reasons for which are a matter of speculation. These could be inhomogeneities in the wall rock, such as compositional banding, or perhaps inhomogeneities within the crystallising magma. Eventually this resulted in the formation of individual beads and partial or complete squeezing out of magma from between the beads, leaving behind only a thin connecting seam. The fact that the beads are steep rods and that the steep NS-striking, as well as the horizontal pegmatite dykes are not beaded, suggests that the orientation of the local stress field and/or sedimentary layering played a role (but, as yet unknown) in the establishment of the final bead geometries.

The above model necessitates slow cooling of the pegmatitic magma, as otherwise the magma would quickly freeze and would have no chance to flow after emplacement and to alter the geometry of the arrested dyke. Furthermore, the host rock must be ductile enough, and therefore hot enough, to make space for the beads by ductile flow, before the magma completely solidifies. These conditions appear to be satisfied, both in South Finland and on Cap de Creus, where the pegmatites intruded into hot rocks at temperatures not far from the solidus of the pegmatites, in the perianatectic domain close to anatexis of the metasediments. Large pegmatite intrusions may have taken an extended time to freeze completely, allowing for flow of solidifying magma and the hot and ductile host rock. Thin pegmatitic veins, however, would have frozen faster, which would explain why no beads appear to have formed in veins <5 cm in thickness.

5. Conclusions

Strings of pegmatite lenses and blocks that are found in South Finland and on Cap de Creus appear at first sight to

have formed by boudinaging of pegmatite sheets. They are, however, original emplacement structures that experienced little or no stretching. Thus, the major form and orientation of pegmatites was established during the intrusive stage. The structures arose from redistribution of solidifying magma along intruded sheets, causing local expansion and collapse that was accommodated by ductile deformation of the host rock. This can occur if the host rock is close to the solidus temperature of an intruding magma, so that the magma freezes slowly enough to allow the necessary time for ductile deformation of that host rock. The main characteristics to distinguish magmatic bead strings from boudins are listed in Table 1.

Correct interpretation of the boudin-like structures is of major importance for tectonic analysis. If the bead strings at Cap de Creus are interpreted as boudins, the pegmatite dykes would have stretched and rotated towards a stagnant or rotating foliation (Passchier, 2001). Strain field interpretation would then range from *sinistral* simple shear with a NE–SW-trending shear plane to roughly NW–SE oriented pure shear shortening. Interpretation as non-stretched bead strings, however, indicates a dominant *dextral* shear component with a roughly ESE–WNW shear plane. Therefore, caution must be taken when interpreting these types of structures in order to avoid erroneous tectonic explanations. Especially where transected structures (foliation or layering) are at a high angle to an intruding vein, there should be no problem in distinguishing bead-string and boudinaged veins (Fig. 11). When all are parallel, additional data (e.g. intrusive apophyses in ‘boudin-necks’) are required. This warning can be extrapolated to all metamorphic areas where similar structures in pegmatites or other intrusive rocks are present.

Acknowledgements

We thank Albert Griera and Abdelmejid Rahimi for their help and debate in the field. This project was funded by the German DAAD, project 314/Al-e-dr, and the Spanish

MCYT (projects HA2000-0055 and BTE2001-2616). The Dutch Dr Schürmann Fund for Precambrian Research is thanked for funding fieldwork in Finland. This paper benefited from the comments of Sue Treagus and an anonymous reviewer.

References

- Ábalos, B., Carreras, J., Druguet, E., Escuder Viruete, J., Gómez Pugnare, M.T., Lorenzo Alvarez, S., Quesada, C., Rodríguez Fernández, L.R., Gil-Ibarguchi, J.I., 2002. Variscan and Pre-Variscan Tectonics. In: Gibbons, W., Moreno, T. (Eds.), *The Geology of Spain*, Geological Society, London, pp. 155–183.
- Alfonso, P., Melgarejo, J.C., Yusta, I., Velasco, F., 2003. Geochemistry of feldspars and muscovite in granitic pegmatite from the Cap de Creus field, Catalonia, Spain. *The Canadian Mineralogist* 41, 103–116.
- Autran, A., Fontelles, M., Guitard, G., 1970. Relations entre les intrusions de granitoïdes, l'anatexie et le métamorphisme régional considérées principalement du point de vue du rôle de l'eau; cas de la chaîne hercynienne des Pyrénées Orientales. *Bulletin de la Société Géologique de France* 12, 673–731.
- Barnolas, A., Chiron, J.C., 1996. Synthèse géologique et géophysique des Pyrénées. Vol. 1: Introduction Géophysique—Cycle Hercynien. BRGM-ITGE, Orléans.
- Bons, P.D., van Milligen, B.P., 2001. A new experiment to model self-organized critical transport and accumulation of melt and hydrocarbons from their source rocks. *Geology* 29, 919–929.
- Bons, P.D., Dougherty-Page, J., Elburg, M.A., 2001. Stepwise accumulation and ascent of magmas. *Journal of Metamorphic Geology* 19, 627–633.
- Brisbin, W.C., 1986. Mechanics of pegmatite intrusion. *American Mineralogist* 71, 644–651.
- Carreras, J., 2001. Zooming on Northern Cap de Creus shear zones. *Journal of Structural Geology* 23, 1457–1486.
- Carreras, J., Druguet, E., 1994. Structural zonation as a result of inhomogeneous non-coaxial deformation and its control on syntectonic intrusions: an example from the Cap de Creus area (eastern-Pyrenees). *Journal of Structural Geology* 16, 1525–1534.
- Cloos, E., 1947. Boudinage. *Transactions of the American Geophysical Union* 28, 626–632.
- Damm, K.W., Harmon, R.S., Heppner, P.M., Dornsiepen, U., 1992. Stable isotope constraints of the Cabo de Creus garnet–tourmaline pegmatites, Massif des Alberes, Eastern Pyrenees, Spain. *Geological Journal* 27, 76–86.
- Druguet, E., 1997. The structure of the NE Cap de Creus Peninsula. Ph.D. thesis, Universitat Autònoma de Barcelona.
- Druguet, E., 2001. Development of high thermal gradients by coeval transpression and magmatism during the Variscan orogeny: insights from the Cap de Creus (Eastern Pyrenees). *Tectonophysics* 332, 275–293.
- Druguet, E., Hutton, D.H.W., 1998. Syntectonic anatexis and magmatism in a mid-crustal transpressional shear zone: an example from the Hercynian rocks of the eastern Pyrenees. *Journal of Structural Geology* 20, 905–916.
- Druguet, E., Passchier, C.W., Carreras, J., Victor, P., den Brok, S.W.J., 1997. Analysis of a complex high-strain zone at Cap de Creus, Spain. *Tectonophysics* 280, 31–45.
- Ehlers, C., Lindroos, A., Selonen, O., 1993. The late Svecofennian granite–migmatite zone of southern Finland—a belt of transpressive deformation and granite emplacement. *Precambrian Research* 64, 295–309.
- Emerman, S.H., Marrett, R., 1990. Why dykes? *Geology* 18, 231–233.
- Ghosh, S.H., Sengupta, S., 1999. Boudinage and composite boudinage in superposed deformation and syntectonic migmatization. *Journal of Structural Geology* 21, 97–110.
- Goldstein, A.G., 1988. Factors affecting the kinematic interpretation of asymmetric boudinage in shear zones. *Journal of Structural Geology* 10, 707–715.
- Goscombe, B., Passchier, C.W., 2003. Asymmetric boudins as shear sense indicators—an assessment from field data. *Journal of Structural Geology* 25, 575–589.
- ten Grotenhuis, S.M., Pizolo, S., Pakula, T., Passchier, C.W., Bons, P.D., 2002. Are polymers suitable rock analogs? *Tectonophysics* 350, 35–47.
- Hanmer, S., 1986. Asymmetrical pull-aparts and foliation fish as kinematic indicators. *Journal of Structural Geology* 8, 111–122.
- Lacassin, R., Leloup, P.H., Tapponier, P., 1993. Bounds on strain in large Tertiary shear zones of SE Asia from boudinage restoration. *Journal of Structural Geology* 15, 677–692.
- Lindroos, A., Romer, R.L., Ehlers, C., Alviola, R., 1996. Late-orogenic Svecofennian deformation in SW Finland constrained by pegmatite emplacement ages. *Terra Nova* 8, 567–574.
- Lister, J.R., Kerr, R.C., 1991. Fluid-mechanical models of crack propagation and their application to magma transport in dykes. *Journal of Geophysical Research* 96, 10,049–10,077.
- Mawer, C.K., 1987. Shear criteria in the Grenville province, Ontario, Canada. *Journal of Structural Geology* 9, 531–539.
- Passchier, C.W., 2001. Flanking structures. *Journal of Structural Geology* 23, 951–962.
- Petford, N., Kerr, R.C., Lister, J.R., 1993. Dike transport of granitoid magmas. *Geology* 21, 845–848.
- Petford, N., Cruden, A.R., McCaffrey, K.J.W., Vigneresse, J.-L., 2000. Granite formation, transport and emplacement in the Earth's crust. *Nature* 408, 669–673.
- Pizolo, S., ten Grotenhuis, S.M., Passchier, C.W., 2001. A new apparatus for controlled general flow modeling of analog materials. In: Koyi, H.A., Mancktelow, N.S. (Eds.), *Tectonic Modeling: A Volume in Honor of Hans Ramberg*. Geological Society of America Memoir 193, pp. 235–244.
- Price, N.J., Cosgrove, J.W., 1990. *Analysis of Geological Structures*. Cambridge University Press, Cambridge.
- Ramberg, H., 1955. Natural and experimental boudinage and pinch-and-swell structures. *Journal of Geology* 63, 512–526.
- Ramsay, J.G., 1967. *Folding and Fracturing of Rocks*. McGraw Hill, New York.
- Rubin, A.M., 1993. Dikes vs. diapirs in viscoelastic rock. *Earth and Planetary Science Letters* 117, 653–670.
- Sederholm, J.J., 1926. On migmatites and associated pre-Cambrian rocks of southwestern Finland, Part II. The region around the Barösundsfjärd W of Helsingfors and neighbouring areas. *Bull. Comm. Geol. Finl.* 77, 143.
- Spence, D.A., Turcotte, D.L., 1985. Magma-driven propagation of cracks. *Journal of Geophysical Research* 90, 575–580.
- Swanson, M.T., 1992. Late Acadian–Alleghenian transpressional deformation: evidence from asymmetric boudinage in the Casco Bay area, coastal Maine. *Journal of Structural Geology* 14, 323–341.
- Weijermars, R., 1986. Flow behaviour and physical chemistry of bouncing putties and related polymers in view of tectonic laboratory applications. *Tectonophysics* 124, 325–358.
- Weinberg, R.F., 1999. Mesoscale pervasive felsic magma migration: alternatives to dyking. *Lithos* 46, 393–410.